

# TI Designs: TIDA-020008 汽车电动座椅参考设计



## 说明

该设计提供了用于使用双向和单向电机驱动器的电机驱动应用（如汽车电动座椅）的驱动和控制电路。它演示了如何驱动具有小电路板尺寸、高度可靠性和完整诊断功能的刷式直流电机。该设计说明了用于增加电机驱动舒适性和便利性选项以及使用更智能的全功能器件替代基于继电器的电路的解决方案。

## 资源

<a href="#">TIDA-020008</a>	设计文件夹
<a href="#">DRV8703-Q1</a>	产品文件夹
<a href="#">DRV8873-Q1</a>	产品文件夹
<a href="#">TPS2H160-Q1</a>	产品文件夹
<a href="#">TPS22810-Q1</a>	产品文件夹
<a href="#">SN74LV4051A-Q1</a>	产品文件夹
<a href="#">TLIN1029-Q1</a>	产品文件夹
<a href="#">TPS7B82-Q1</a>	产品文件夹



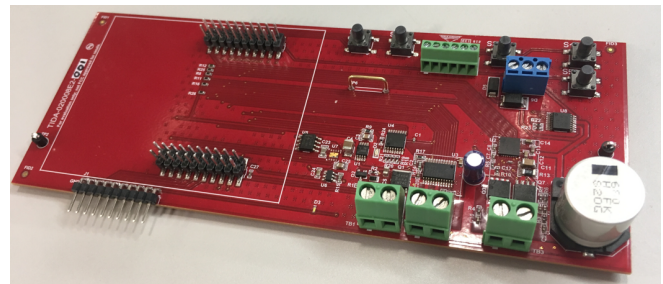
咨询我们的 E2E™ 专家

## 特性

- 用于直流电机的双向驱动器
  - 刷式电机 A: 高达 30A 峰值
  - 刷式电机 B: 高达 10A 峰值
- 用于腰托的单向驱动器
  - BDC 泵电机
  - 电磁阀
- 来自所有电机的多路复用电流感应信号
- 反向电池保护和负载突降保护
- 每个驱动电路的小电路板尺寸

## 应用

- [座椅位置和舒适模块](#)
- [座椅位置和折叠模块](#)
- [座椅舒适模块](#)



该 TI 参考设计末尾的重要声明表述了授权使用、知识产权问题和其他重要的免责声明和信息。

## 1 System Description

The TIDA-020008 reference design implements drive, control, and diagnostic circuits applicable to several features found in automotive power seats. Three different drive topologies demonstrate how to design for a variety of system requirements with a high degree of adjustability to match the wide range of automotive body features found in a power seat (or similar applications).

- High-current (up to 30-A peak) bidirectional brushed DC (BDC) motor drive
- Medium-current (up to 10-A peak) bidirectional brushed DC motor drive
- Dual single-direction drive for actuators such as solenoids or unidirectional pumps or fans

The design also implements the ancillary functions needed for a power seat module, such as power conditioning, network communications, and illumination control.

The design includes an example of a high-current bidirectional motor drive using a solid-state full-bridge circuit. Based around the DRV8703-Q1 motor driver, this circuit includes all the components needed for driving motors up to around 300 W of peak power (30 A at typical automotive battery voltages). It also includes smart drive features IDRIVE and TDRIVE to facilitate tuning the motor operation for improved efficiency and EMC performance. Diagnostic features monitor the motor current and state of the final drive FETs to provide real-time feedback of the critical drive conditions. This high-current bidirectional drive is intended for and tested with typical power seat motorized features such as seat positioning for forward and back, up and down, and seat tilt.

The medium-current drive includes all the components needed for driving motors with up to 10 A of peak current, using the single-chip DRV8873-Q1 motor driver. It includes register-programmable features to adjust the off-time and slew rate of the drive stage to improve efficiency and EMC performance. Diagnostic features monitor the motor current and state of the drive FETs to provide real-time feedback of the critical drive conditions, including detection of faults such as supply undervoltage, charge pump undervoltage, motor overcurrent, open load, and high-temperature thermal faults. This circuit is intended for and tested with power seat features such as motorized headrest adjust or similar bidirectional adjustments.

A dual-channel smart high-side switch implements the control and drive circuits for single-directional motorized applications such as lumbar support inflation pumps and the associated solenoid valves with spring return. The features of this circuit include an adjustable current limit to protect against short-to-ground load faults, thermal shutdown, and protection against negative voltage spikes caused by inductive loads.

An eight-channel multiplexer allows selecting any of several different signals to monitor with a single microcontroller analog-to-digital converter (ADC), simplifying the MCU requirements while still providing full diagnostic capabilities. A low-power mode is implemented to allow reducing the overall current from the battery to a very low level during periods when adjustment of the seat is not active.

A thermally-protected load switch provides a simple LED drive circuit for turning on an onboard LED to illuminate under the seat; alternately an off-board LED can be driven by the same circuit. A standard LaunchPad™ interface to an off-board microcontroller provides common signals for monitoring and control of the drives. The entire design is protected against reverse-battery conditions and load-dump conditions, and includes a LIN transceiver for communication with a central Body Control Module (BCM).

## 1.1 Key System Specifications

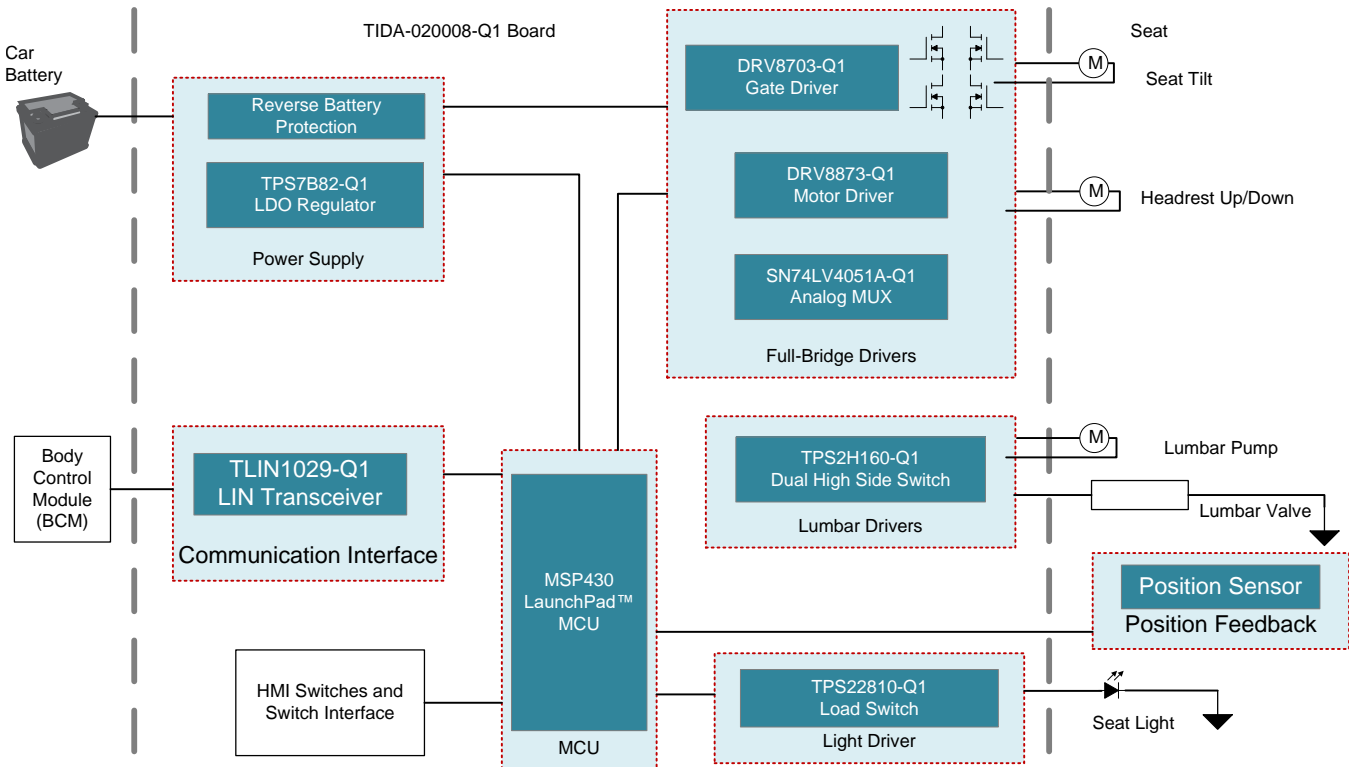
表 1. Key System Specifications

PARAMETER	SPECIFICATIONS	DETAILS
Drive A motor type	Bidirectional brushed DC motor	<a href="#">节 2.4.1</a>
Drive A peak current	30 A	
Drive B motor type	Bidirectional brushed DC motor	<a href="#">节 2.4.2</a>
Drive B peak current	10 A	
Drive C motor type	Unidirectional brushed DC motor	<a href="#">节 2.4.3</a>
Drive C peak current	4 A	
Drive D motor type	DC solenoid valve	<a href="#">节 2.4.3</a>
Operating supply voltage range	6 V to 18 V	
Survivable supply voltage range	-20 V to 40 V	
Peak total drive current	40 A	
Sleep-mode quiescent current	< 100 $\mu$ A	
Position feedback compatibility	Hall effect sensor inputs or ripple count	<a href="#">节 2.4.7</a>
Current sense	Selectable by multiplexer	
Microcontroller interface	LaunchPad 2 $\times$ 20-pin connectors	<a href="#">节 2.4.8</a>
Network connectivity	LIN Transceiver	<a href="#">节 2.3.5</a>
Illumination circuit	Thermally-protected LED switch	

## 2 System Overview

### 2.1 Block Diagram

图 1. TIDA-020008 Block Diagram



### 2.2 Design Considerations

To simplify this reference design and make the design more adaptable to a variety of microcontroller units (MCUs), the board is implemented in the BoosterPack™ format. This board format has a simple connector interface to the external LaunchPad MCU board, which allows this reference design to be evaluated with a wide selection of MCUs. The LaunchPad plus BoosterPack implementation also has the advantage that code development and design testing are facilitated with existing tools such as Code Composer Studio™ or Energia, thus speeding up optimization of the design for any specific operating conditions. While the BoosterPack format does allow flexibility in using different MCU boards, the format also creates constraints on the size and layout of the board. In a production version of this design, the MCU would likely be installed on the same board with the chips and other components with a significant reduction in board size.

For ease of testing, the board includes five control switches that would not be present in a production power seat module design. These switches provide for user inputs without the need for an external network or computer.

Another consideration is selecting the passive components. In general, components are selected based on the performance requirements of the expected applications. Where practical, components with automotive ratings are selected. For active components, the components selected are AEC-Q100 qualified to either temperature grade 0 or temperature grade 1.

Capacitors are generally X7R grade ( $-55^{\circ}\text{C}$  to  $+125^{\circ}\text{C}$ ) or higher with size and value selected for the expected extremes of operation conditions. The voltage rating of the capacitors must be greater than the maximum voltage they could experience and two times the typical operating voltage to avoid DC bias effects. The amount of output capacitance used depends on output ripple and transient response requirements, and many equations and tools are available online to help estimate these values.

## 2.3 Highlighted Products

### 2.3.1 DRV8703-Q1 Automotive H-Bridge Gate Driver

The DRV8703-Q1 is a single H-bridge gate drivers that use four external N-channel MOSFETs targeted to drive a bidirectional brushed-DC motor.

A PH/EN, independent H-Bridge, or PWM interface allows simple interfacing to controller circuits. An internal sense amplifier provides adjustable current control. Integrated Charge-Pump allows for 100% duty cycle support and can be used to drive external reverse battery switch.

Independent half-bridge mode allows sharing of half bridges to control multiple DC motors sequentially in a cost-efficient way. The gate driver includes circuitry to regulate the winding current using fixed off-time PWM current chopping.

The DRV8703-Q1 includes Smart Gate Drive technology to remove the need for any external gate components (resistors and Zener diodes) while fully protecting the external FETs. The Smart Gate Drive architecture optimizes dead time to avoid any shoot-through conditions, provides flexibility in reducing electromagnetic interference (EMI) with programmable slew-rate control and protects against any gate-short conditions. Additionally, active and passive pulldowns are included to prevent any  $dv/dt$  gate turnon.

A low-power sleep mode is provided which shuts down internal circuitry to achieve a very-low quiescent-current draw. The device can be used in a very compact design because of its small 5 mm  $\times$  5 mm package with few external components.

### 2.3.2 DRV8873-Q1 Automotive H-Bridge Motor Driver

The DRV8873-Q1 device is an integrated driver IC for driving a brushed DC motor in automotive applications. Two logic inputs control the H-bridge driver, which consists of four N-channel MOSFETs that drive motors bidirectionally with up to 10-A peak current. The device operates from a single power supply and supports a wide input supply range from 4.5 V to 38 V.

A PH/EN or PWM interface allows simple interfacing to controller circuits. Alternatively, independent half-bridge control is available to drive two solenoid loads.

A current mirror allows the controller to monitor the load current. This mirror approximates the current through the high-side FETs, and does not require a high-power resistor for sensing the current.

A low-power sleep mode is provided to achieve very-low quiescent current draw by shutting down much of the internal circuitry. Internal protection functions are provided for undervoltage lockout, charge pump faults, overcurrent protection, short-circuit protection, open-load detection, and overtemperature. Fault conditions are indicated on an nFAULT pin and through the SPI registers.

### 2.3.3 TPS2H160-Q1 Dual-channel Smart High-side Switch

The TPS2H160-Q1 is a fully-protected dual-channel smart high-side switch, with integrated 160-m $\Omega$  NMOS power FETs.

Full diagnostics and high-accuracy current-sense features enable intelligent control of the load.

An external adjustable current limit improves reliability of the whole system by limiting the inrush or overload current.

### 2.3.4 TPS22810-Q1 Load Switch

The TPS22810-Q1 is a one channel load switch with configurable rise time and integrated quick output discharge (QOD). The device features thermal shutdown to protect the device against high junction temperature and thereby ensure safe operating area of the device inherently. The device features a N-channel MOSFET that can operate over an input voltage range of 2.7 V to 18 V. The device can support a maximum current of 2 A. The switch is controlled by an on and off input that can interface directly with low-voltage control signals.

The configurable rise time of the device greatly reduces inrush current caused by large bulk load capacitances, thereby reducing or eliminating power supply droop. Undervoltage lock-out is used to turn off the device if the  $V_{IN}$  voltage drops below a threshold value, ensuring that the downstream circuitry is not damaged from being supplied by a voltage lower than intended. The configurable QOD pin controls the fall time of the device to allow design flexibility for power down.

### 2.3.5 TLIN1029-Q1 LIN Transceiver

The TLIN1029-Q1 is a *Local Interconnect Network* (LIN) physical layer transceiver with integrated wake-up and protection features, compliant to LIN 2.0, LIN 2.1, LIN 2.2, LIN 2.2A and ISO/DIS 17987–4.2 standards. LIN is a single wire bidirectional bus typically used for low speed in-vehicle networks using data rates up to 20 kbps. The TLIN1029-Q1 is designed to support 12-V applications with wider operating voltage and additional bus-fault protection. The LIN receiver supports data rates up to 100 kbps for in-line programming. The TLIN1029-Q1 converts the LIN protocol data stream on the TXD input into a LIN bus signal using a current-limited wave-shaping driver which reduces electromagnetic emissions (EME). The receiver converts the data stream to logic level signals that are sent to the microprocessor through the open-drain RXD pin. Ultra-low current consumption is possible using the sleep mode which allows wake-up via LIN bus or pin. The integrated resistor, ESD and fault protection allows designers to save board space in their applications.

### 2.3.6 TPS7B69-Q1 Linear Voltage Regulator

The TPS7B69xx-Q1 device is a low-dropout linear regulator designed for up to 40-V VI operations. With only 15- $\mu$ A (typical) quiescent current at light load, the device is suitable for standby microcontrol-unit systems especially in automotive applications.

The devices feature an integrated short-circuit and overcurrent protection. The TPS7B69xx-Q1 device operates over a  $-40^{\circ}\text{C}$  to  $125^{\circ}\text{C}$  temperature range. Because of these features, the TPS7B6925-Q1, TPS7B6933-Q1, and TPS7B6950-Q1 devices are well suited in power supplies for various automotive applications.

### 2.3.7 SN74LV4051A-Q1 Eight-channel Multiplexer

This 8-channel CMOS analog multiplexer and demultiplexer is designed for 2-V to 5.5-V VCC operation.

The SN74LV4051A handles analog and digital signals. Each channel permits signals with amplitudes up to 5.5 V (peak) to be transmitted in either direction.

Applications include signal gating, chopping, modulation or demodulation (modem), and signal multiplexing for analog-to-digital and digital-to-analog conversion systems.

## 2.4 System Design Theory

The overall TIDA-020008 design consists of several circuits which operate effectively as independent functions. Each functional circuit is discussed in this section, and test results are presented in 3.2 节.

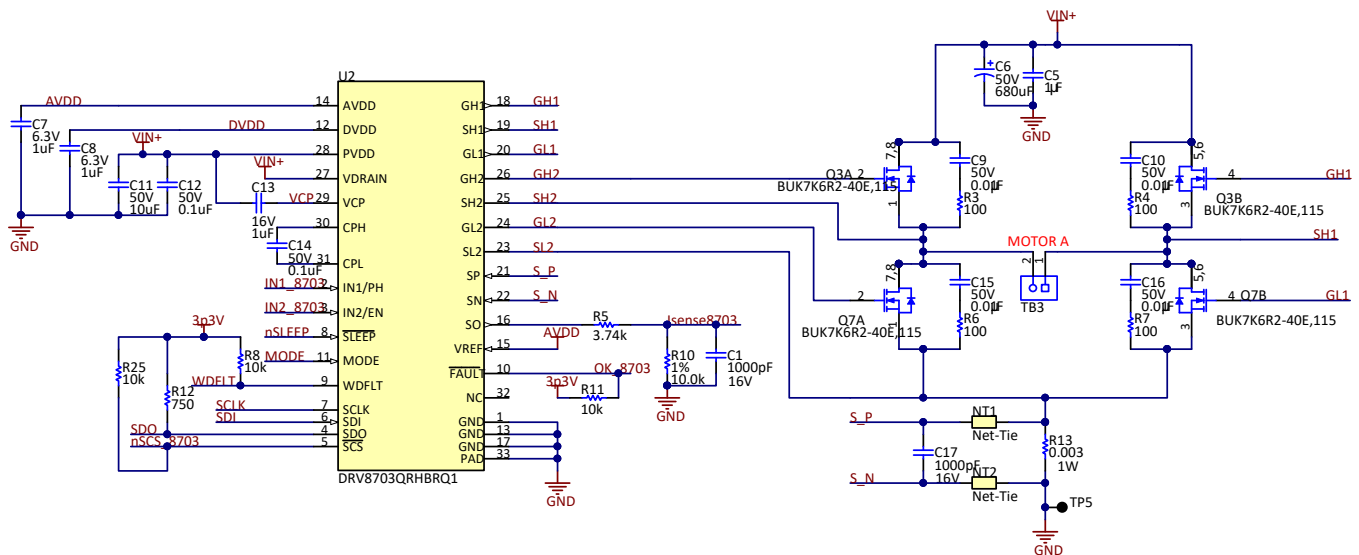
### 2.4.1 High-Current Motor Drive A

In automotive power seat applications, it is common to have relatively powerful motors, with continuous operating current of several amps, and stall current of 10 A or more. For these motors, a smart gate driver and external FETs is a desirable design choice. 图 2 shows the complete electrical schematic for the high-current motor drive circuit, based on the DRV8703-Q1.

The drive stage transistors Q3 and Q7 are dual N-channel enhancement-mode MOSFETs. The BUK9K6R2-40E is rated for up to 40 V across the drain to source connections, to survive overvoltage conditions which may be caused by a load-dump fault. The drain to source on resistance is specified as typically 5.27 mΩ and a maximum of 6.2 mΩ.

The arrangement of the transistors in the full-bridge (or H-bridge) is such that when applying a drive voltage to the motor, only one transistor in each package (Q3, Q7) is in the on state. This serves to spread out the thermal power being dissipated when the motor is active.

图 2. Motor Drive A Schematic, up to 30-A Peak Current



The large bulk capacitor C6 serves as a local reservoir for the current to the motor, supplying the initial transient when the drive stage is activated. The tuning components across the drain to source of each transistor (C9, C10, C15, C16, R3, R4, R6, R7) are not needed due to the ability to adjust the DRV8703-Q1 gate drive currents for both source and sink levels. These components are included for designers who may want to compare the performance using discrete components to shape the transistor waveform with the performance using the smart gate drive capabilities.

The resistor R13 serves as a current sense resistor; whenever the motor is driven, current through the low-side of the H-bridge returns to ground through this resistor. With a value of 3 mΩ, the scale factor is 3 millivolts per amp of motor current. The power rating of 1 W allows continuous motor currents of more than 15 A. If higher currents need be monitored, a lower value of resistance can be selected.

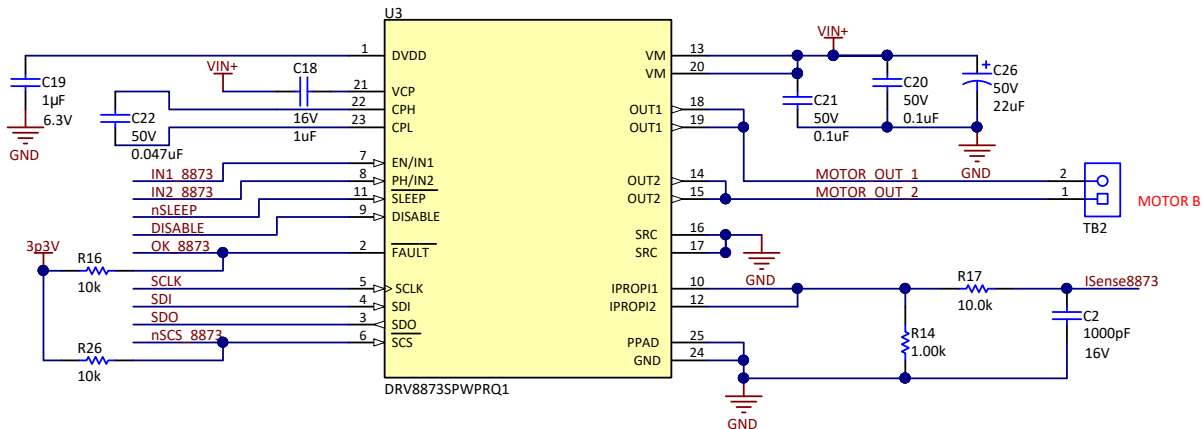
The net-ties NT1 and NT2 are used to keep the schematic editor from routing the low-side sense line S\_N directly to the ground plane. That is, NT2 allows the definition of a new electrical node S\_N which is tied to the ground plane, but which can be routed, along with S\_P, as a Kelvin connection for accurate sensing of the voltage across R13.

The signals S\_P and S\_N are connected to SP and SN pins of the DRV8703-Q1. Internally a differential current sense amplifier (CSA) increases the magnitude of the voltage across R13. The resulting signal on the Sense Output (SO) pin is connected to a resistor divider network formed by R5 and R10, with filter capacitance C1. The value of these components gives ISense8703 a scale factor of about 43 mV per amp of motor current, with an RC time constant of 10 microseconds. Depending on the specific requirements of the application, designers may want to adjust these parameters.

### 2.4.2 Medium Current Motor Drive B

For lower-current applications, such as headrest height or position adjustment, a full-bridge driver with integrated FETs is a good design choice. 图 3 shows the complete schematic for a full-bridge driver with 10-A peak current capability using the DRV8873-Q1. This device integrates the pre-drive circuits, final drive stages, current sense, as well as diagnostic and control circuits into a single compact package.

图 3. Motor Drive B Schematic, up to 10 Amp Peak Current



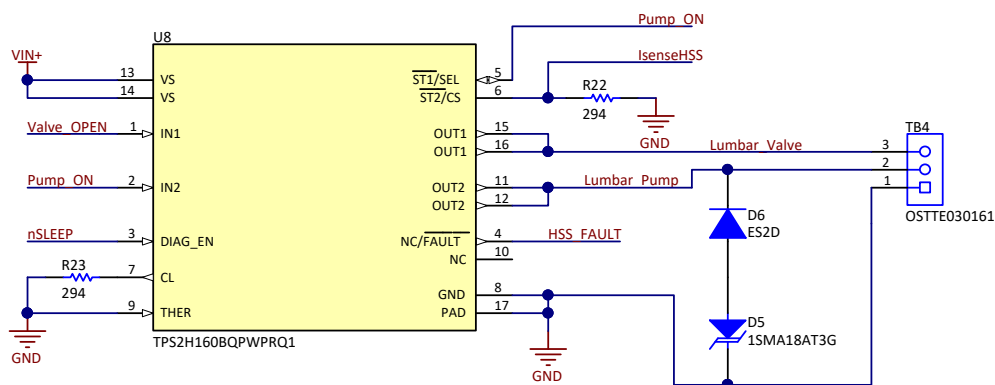
### 2.4.3 Drive Circuits C and D

Some power seat applications do not require the bidirectional drive capabilities of a full-bridge (H-bridge) drive stage. For example, lumbar support features often use a single-direction pump to inflate a pneumatic bladder, with a spring-return solenoid valve to hold the bladder pressure when neither inflating nor deflating the support. Both the pump and the valve can be driven independently using a dual smart high-side switch such as the TPS2H160-Q1, as 图 4 shows.

Resistor R22 sets the scale factor of the current sense output CS. The current-sense ratio of the TPS1H160-Q1 is specified as typically 290 A/A. So the value of 294 Ω of R22 gives a current sense scale factor of about 1 V per Amp of drive current. For the 3.3-V microcontroller used for this design (MSP430), this gives a total range of 3.3 Amps of output current. The linear range of output current is specified for the TPS2H160-Q1 as 0 to 2.5 A, which gives considerable margin beyond the expected operating currents for the typical test loads.

Resistor R23 sets the current limit for both channels of the TPS2H160-Q1. The typical scale factor for the CL pin current is 2500 times smaller than the output current, and the typical current limit threshold is 0.8 V. So a CL pin current of  $0.8 \text{ V} / 294 \Omega = 2.7 \text{ mA}$  reaches the current limit threshold; this corresponds to an output current of  $2500 \times 2.7 \text{ mA} = 6.8 \text{ A}$ .

图 4. Drive C and D Schematic Diagram



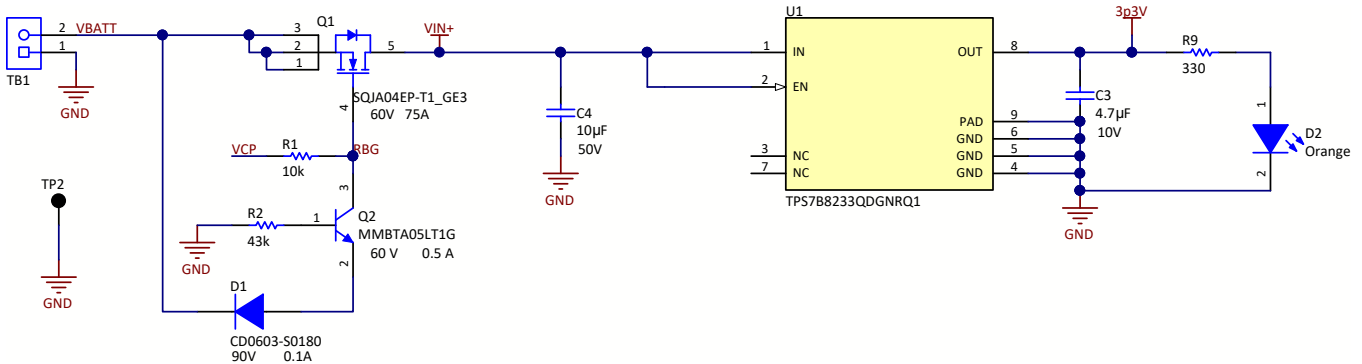
The arrangement of the lumbar pump and valve used for testing allowed use of the Pump\_ON signal to select between monitoring the *Lumbar Pump* or the *Lumbar Valve*, in terms of current sense and current limit. When inflating the lumbar bladder, the lumbar pump supplies compressed air through the actively-opened lumbar valve, so both output channels are active, and a logic-high Pump\_ON signal selects OUT2 (*Lumbar\_Pump*) to be monitored. When deflating the lumbar bladder, the lumbar valve is open, but the lumbar pump is off, and a logic-low Pump\_ON signal selects OUT1 (*Lumbar\_Valve*) to be monitored. When the bladder is holding pressure, not being inflated nor deflated, both output are off, and the spring-return solenoid valve is closed.

The TPS2H160-Q1 is specified for inductive load switch-off energy up to 40 mJ. This is the energy stored in the active motor coil, or solenoid coil, that must be dissipated when the load is switched off; sometimes called the "inductive kick". For the test loads used to demonstrate the performance of this circuit, the inductive turn-off energy did not exceed this level, so no external protection is needed. However, clamping diodes D5 and D6 are included in the board layout to accommodate loads with inductive loads that do exceed 40 mJ.

## 2.4.4 Power Supply

The power supply circuit in 图 5 includes a linear low-drop out (LDO) voltage regulator U1, reverse battery protection, as well as an LED used for testing to indicated the 3.3-V supply is active.

图 5. Power Supply Schematic



#### 2.4.4.1 Reverse Battery Protection

When the polarity of the applied battery voltage (VBATT) is positive with respect to GND, current can pass through the body diode of transistor Q1 to VIN+, supplying U2, the DRV8703-Q1, with sufficient supply to operate, see 节 2.4.1. If the nSLEEP signal is asserted (logic high), then the U2 charge pump voltage VCPF is several volts higher than VIN+. As VCPF is applied to the gate of Q1, the transistor is turned on, reducing the voltage drop from VBATT to VIN+ and allowing the design board to be fully powered. If the nSLEEP signal is not asserted (logic low), the U2 charge pump is inactive, and Q1 will not be on. Therefore, when nSLEEP is not asserted, there is a voltage drop from VBATT to VIN+ due to the body diode of Q1. This drop will not cause any significant power dissipation issues because the current when nSLEEP is logic low should be very small. During normal (positive) VBATT polarity, the base of Q2 is at GND, and Q2 is off, having no effect on the circuit.

When the polarity of the applied battery voltage VBATT is negative with respect to GND, the body diode of Q1 blocks any current flow from VBATT to VIN+. To ensure that Q1 is off, the bipolar NPN transistor Q2 is turned on by a base current flowing from GND through R2. Whenever the voltage at VBATT is more negative with respect to GND than two diode drops (VBE of Q2 plus the forward drop of D1), then Q2 is on and pulls the gate of Q1 to a negative value.

#### 2.4.4.2 Linear Voltage Regulator

The power supply converts the 12-V automotive battery voltage to the 3.3-V supply needed by the microcontroller and the other components. The requirements for the power supply circuit are to produce a stable 3.3-V supply capable of at least 35 mA, while surviving electrical conditions such as reverse-battery and load-dump. The TPS7B8233-Q1 provides regulation of a fixed 3.3-V supply and has a wide survivable input voltage range up to 45 V. The TPS7B8233-Q1 device is stable with ceramic output capacitors, which is preferred for automotive applications.

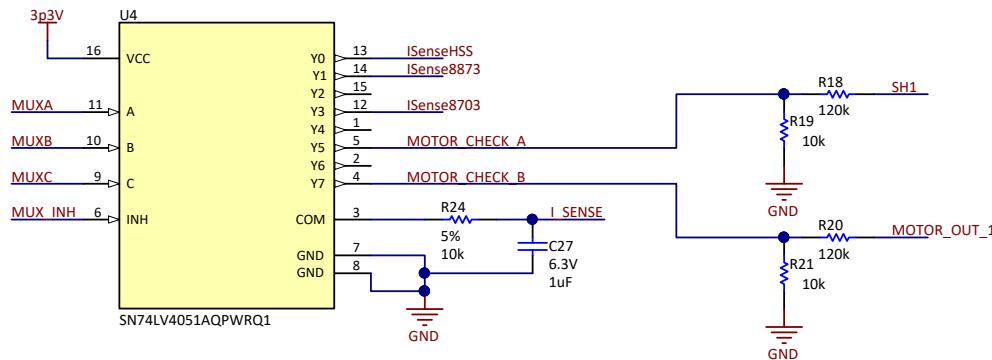
The input capacitor C4 has a capacitance value of 10 µF in accordance with the guidance in [TPS7B82-Q1 High-Voltage Ultralow- \$I\_q\$  Low-Dropout Regulator](#). The voltage rating of C4 is 50 V to allow overvoltage conditions such as load dump without damage to the capacitor. The output capacitor C3 has a capacitance value of 4.7 µF in accordance with the guidance in the TPS7B82-Q1 data sheet. The light-emitting diode (LED) D2 is a visual indicator that the 3.3-V supply is operating

### 2.4.5 Analog Multiplexer Circuit

图 6 shows the analog multiplexer circuit. This circuit allows a single microcontroller ADC channel to monitor several current and voltage feedback signals throughout the power seat drive. The SN74LV4051A-Q1 has 8 selectable input channels multiplexed to one output channel. The switch resistance for these channels is less than 600 Ω under all conditions, and channel-to-channel matching is better than 40 Ω. These low resistance values allow for consistent performance with the RC low-pass filter formed by R24 and C27, without significant variation due to switch resistance.

The values of R24 and C27 give an RC time constant of 10 milliseconds; designers should consider the frequencies of interest for their particular feedback control and diagnostic requirements.

图 6. Analog Multiplexer Schematic



In this design, only five of the eight channels are used; in a full power seat design, additional channels would be used to monitor the signals associated with additional motor drives. By setting the MUXA, MUXB, and MUXC signals, the microcontroller ADC can monitor:

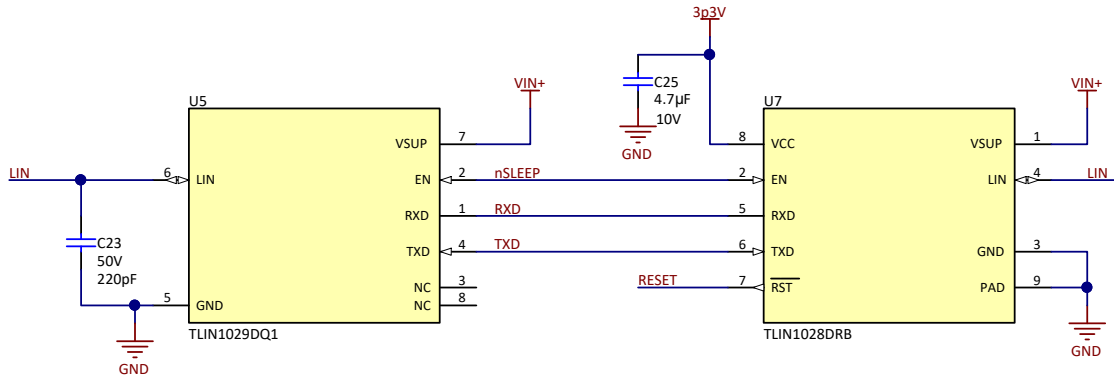
- I\_SenseHSS - the current sense signal from the dual-channel smart high-side switch. In this design, when the lumbar pump is inflating the lumbar support, I\_SenseHSS is a scaled version of the lumbar pump motor current. When the lumbar support is being deflated, I\_SenseHSS is a scaled version of the lumbar valve solenoid current.
- I\_Sense8873 - the current sense signal from the DRV8873-Q1, which in our testing was used to drive the headrest height adjustment motor.
- I\_sense8703 - the current sense signal from the DRV8703-Q1, which in our testing was driving the motors which adjusted the power seat height, forward and back position, or seat tilt.
- MOTOR\_CHECK\_A - the voltage to the high-current motor connected to Motor Drive A. Resistors R18 and R19 scale the expected voltage range on SH1 to the 3.3-V range of the LaunchPad ADC.
- MOTOR\_CHECK\_B - the voltage to the medium-current motor connected to Motor Drive B. Resistors R20 and R21 scale the expected voltage range on MOTOR\_OUT\_1 to the 3.3-V range of the LaunchPad ADC.

Depending on the requirements and diagnostic features designed in any specific design, designers can connect the various channels to

### 2.4.6 LIN Transceiver Circuit

图 7 展示了 LIN 收发器电路。TLIN1029-Q1 是一个独立的 LIN 收发器，将 LIN 物理层总线上的信号转换为逻辑电平信号。电源座模块通常是 LIN 总线上的从节点；远程 LIN 主节点，如 *Body Control Module*，通常包含 LIN 总线上的 1-kΩ 上拉电阻。TLIN1029-Q1 的使能引脚 (EN) 连接到 nSLEEP 信号，该信号将 TIDA-020008 板上的设备置于低功耗睡眠模式，当 nSLEEP 处于逻辑低电平时。

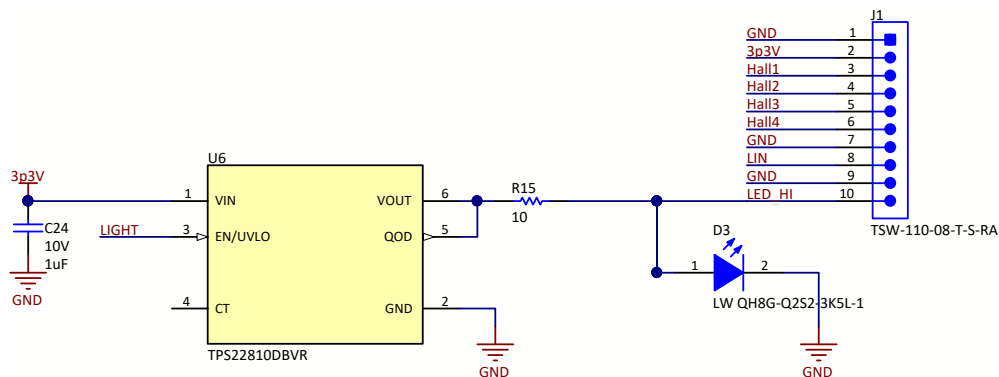
图 7. LIN Transceiver Schematic



### 2.4.7 LED Output and Hall Effect Inputs

图 8 展示了 LED 控制电路和 LIN 通信总线接口连接器，以及输入信号，以便添加霍尔效应传感器（如 DRV5xxx-Q1 系列）用于位置反馈。

图 8. LED Output and Hall Effect Input Schematic



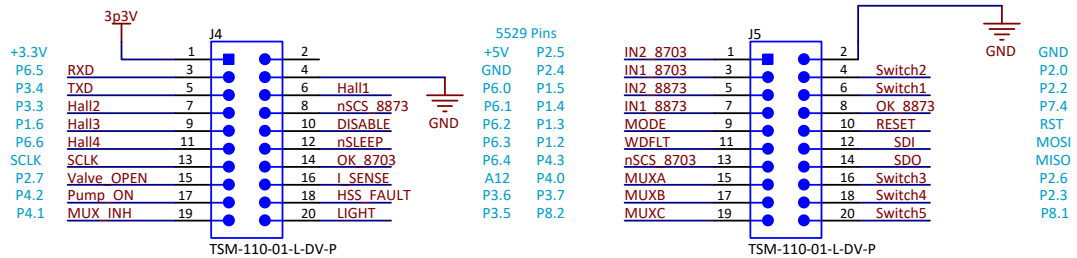
The LED D3 is selected to have a relatively low turn-on voltage, allowing current-limiting resistor R15 to be used in series with the LED.

The four Hall effect inputs provide signals which can be monitored by the microcontroller as part of the motion control loop for each axis. One example of an application using the Hall effect signal is discussed in 节 3.2.2.3.

### 2.4.8 Microcontroller Interface

图 9 显示了用于将 TIDA-020008 板连接到 LaunchPad 微控制器板的连接器。对于 3.2 节中描述的测试，基于 MSP430F5529 微控制器的 MSP430 LaunchPad 提供了 3.1.2 节中描述的输入和输出控制的解释。

图 9. Microcontroller Interface Schematic

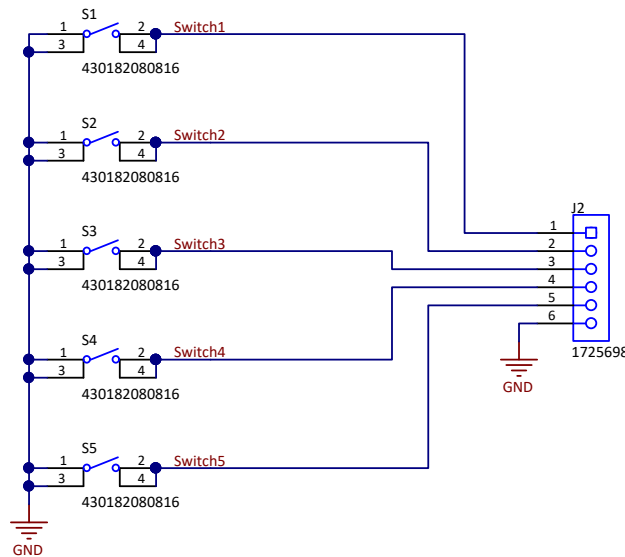


如果设计者想要用不同的微控制器来评估此设计，相同的输入、输出和电源连接可以使用，请记住 TIDA-020008 板是为 3.3-V 微控制器设计的。模拟到数字的缩放和通用 I/O (GPIO) 信号可以修改以适应 5-V 微控制器，如果这是所需的。

### 2.4.9 Test Switch Inputs

图 10 显示了包含在板设计中的推按钮开关，以方便测试。按下每个开关会在对应的 Switch 信号上创建到地的信号路径。当未按下时，开关在对应的 Switch 信号上呈现开路。每个开关信号输入上的 GPIO 引脚上的微控制器都分配了可编程的上拉电阻。

图 10. Switch Input Schematic



在生产座椅模块中，控制座椅功能的开关很可能位于单独的面板上，或实现为显示屏上的可编程开关。

### 2.4.10 Quiescent Current

For automotive body electronics applications, quiescent current is of interest, because the modules which control the functions such as seat adjustments are idle for a large percentage of the time. Low current consumption is necessary so the automotive battery is not drained during long periods of idleness.

表 2 shows the specifications for the devices used in this design. Each device has a low-power mode, with very low quiescent current.

表 2. Quiescent Current (mA)

DEVICE	TYPICAL	MAX I <sub>q</sub> @ 25°C	MAX I <sub>q</sub> @ 125°C	SUPPLY
DRV8703-Q1		14	25	VIN+ (12 V)
DRV8873-Q1	15	30		VIN+ (12 V)
TPS7B82-Q1	2.7	5	5	VIN+ (12 V)
TPS2H160-Q1		0.5	5	VIN+ (12 V)
TPS22810-Q1	0.5	2.3	3.8	3p3V (3.3 V)
SN74LV4051-Q1		20	40	3p3V (3.3 V)
TLIN1029-Q1	8	12		VIN+ (12 V)
<b>Total</b>		<b>83.8</b>		

The VIN+ supply is originated from the VBATT input, coming from the 12-V nominal automotive battery system. The VIN+ is the electrical node after the VBATT supply has gone through the Q1 reverse-battery protection FET, as 图 5 shows.

While two of the devices are supplied by the TPS7B82-Q1 linear voltage regulator, this current still originates as current provided by the VBATT. The total quiescent current for the TIDA-02008 board is less than 100  $\mu$ A, if the LED is disabled by removing resistor R9. The LaunchPad microcontroller board requires additional current from the 3.3-V supply.

## 3 Hardware, Software, Testing Requirements, and Test Results

### 3.1 Required Hardware and Software

#### 3.1.1 Hardware

This design is intended for use in automotive power seats, with applications such as (but not limited to):

- Seat forward and back motion
- Seat up and down motion
- Seat cushion tilt
- Seat back tilt
- Headrest up and down position
- Lumbar support inflate and deflate

The motors and mechanical assemblies for these functions vary across different car models, so a variety of motors was used for testing the design. While being in no way a comprehensive survey of these motors, the test results presented here are intended to give the design insight into performance with a broad range of brushed DC motors.

The motors listed in 表 3 are representative of motors commonly found in automotive power seats.

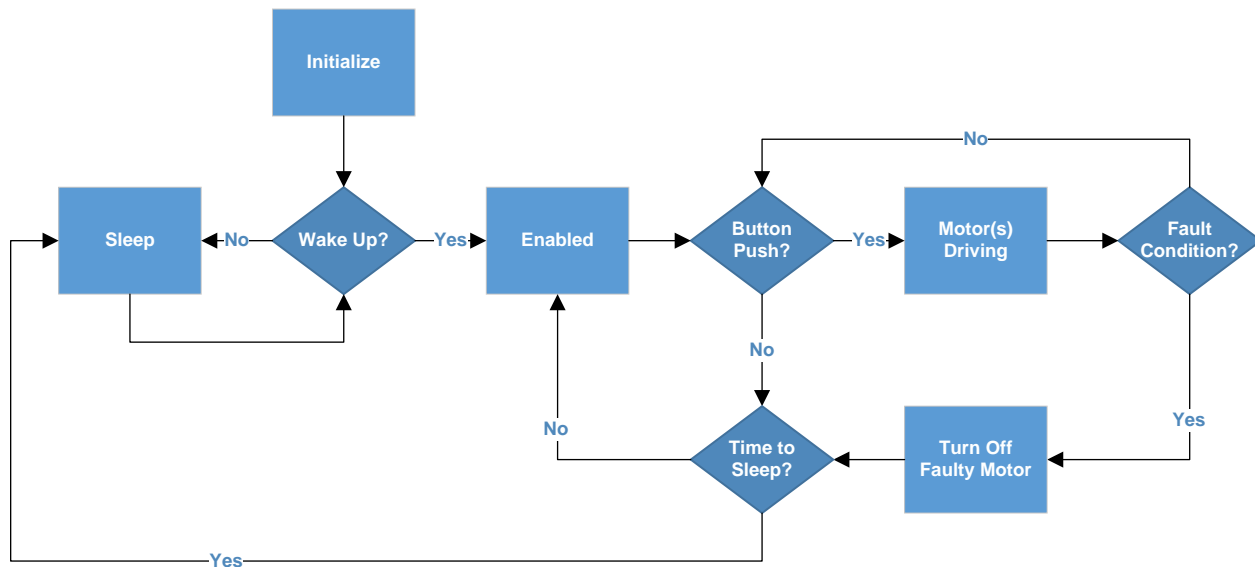
**表 3. Motor Hardware Used for Testing**

MOTOR	WINDING RESISTANCE ( $\Omega$ )	WINDING INDUCTANCE (mH)	STALL CURRENT (A)	TYPICAL OPERATING CURRENT (A)	ELECTRICAL TIME CONSTANT (ms)
Headrest up or down	3.4	3.82	3.5	0.3	1.1
Seat up or down	1.12	743	10.7	2.5	0.66
Seat forward or back	1.07	992	11.2	2.9	0.93
Seat tilt	1.5	0.88	8	2	0.59
Lumbar pump	1.24	1.47	9.7	1.0	1.2
Lumbar valve	43	48	0.28	0.27	1.1
Window lifter	0.82	0.33	14.6	4	0.4
Windshield wiper	0.68	0.36	18	6	0.53

### 3.1.2 Software

For testing and demonstration purposes, a relatively simple software loop is implemented by the MSP430 LaunchPad. This is illustrated in [图 11](#). After initializing the microcontroller and setting the GPIOs, the software loops while monitoring for a button push.

**图 11. Software Flow Diagram**



When a button is pushed, the microcontroller sets the corresponding GPIO pins to control the actuator associated with the desired action. At this point the analog multiplexer (MUX) is also set to connect the active drive circuit to the ADC of the microcontroller. In testing mode, the actuator is active as long as the button is pushed, unless a fault condition occurs.

If, for example, the motor current exceeds the programmable threshold set by the software, the actuator can be disabled. At this point either the faulted motor can be idle, or reversed, depending on the system requirements.

### 3.2 Testing and Results

#### 3.2.1 Test Setup

Unless otherwise noted, the following tests were performed at room temperature, with VBATT set to a 12-V nominal supply. Various automotive mechanisms are used as test loads for the power seat position adjustment, headrest position adjustment, and lumbar support drive as described in the sections for each type of testing.

#### 3.2.2 Test Results

The test results discussed in the following subsections are representative of the performance with the specific hardware used for testing. When designing, consider the system requirements and expected performance of their specific equipment and test conditions

##### 3.2.2.1 Power Supply Testing

The power supply tests include testing to measure the variation of the 3.3-V supply when the input voltage (VBATT) varies, and measuring the input current when VBATT is negative with respect to GND, which mimics a reverse battery condition.

图 12 shows that the 3.3-V supply is active and well regulated for input voltages on VBATT in the range of 4 V to 16 V. These measurements are recorded with no external load on the reference design board.

图 12. Measured 3.3-V Supply vs. Applied VBATT Voltage

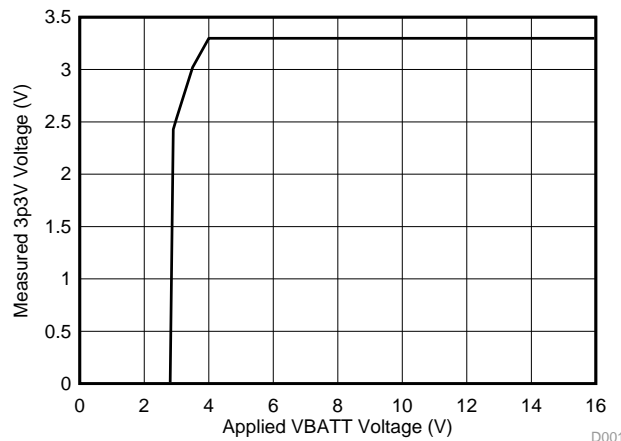
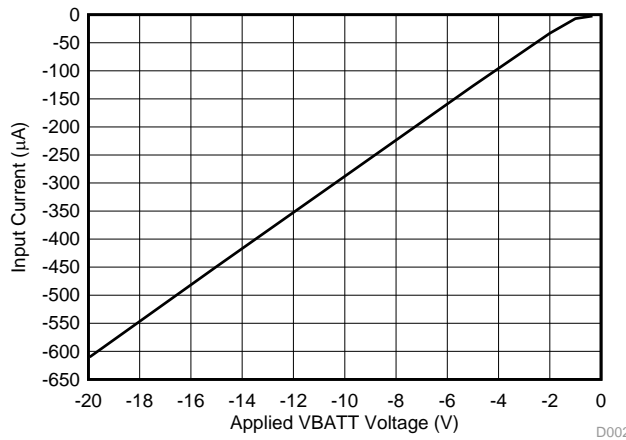


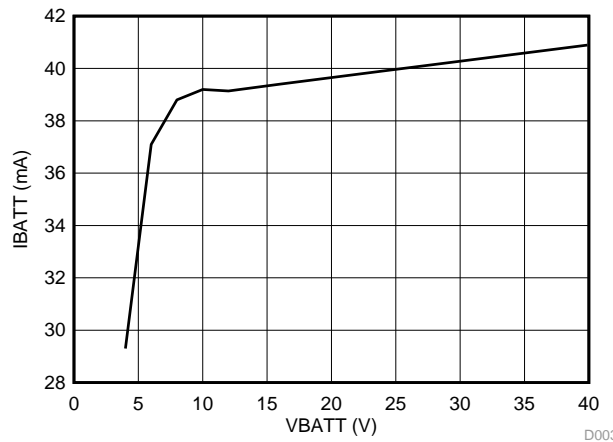
图 13 shows the input current under conditions of negative voltages applied to VBATT (TB1-2) with respect to GND (TB1-1). For applied voltages more negative than -2 V, the current increases linearly, primarily due to the resistor R2 in 图 5.

图 13. Input Current vs. Applied Negative VBATT Voltage



For positive (normal polarity) applied VBATT voltages, 图 14 shows the input current at TB1-2 (VBATT) versus the applied VBATT voltage. For a nominal 12-V VBATT level, the TIDA-020008 design has an input current of around 39 mA, including the LaunchPad microcontroller board. This represents the idle current when no motor is actively being driven, the LIN transceiver is idle, and the illumination LED is off. As the applied voltage is increased to 40 V, there is a slight increase in the input current, but no significant increase. This indicates there is no breakdown of any of the components connected to VBATT, thus the design is not damaged by steady-state VBATT voltages up to 40 V. Thus the design is robust to load-dump conditions that may occur on the battery system.

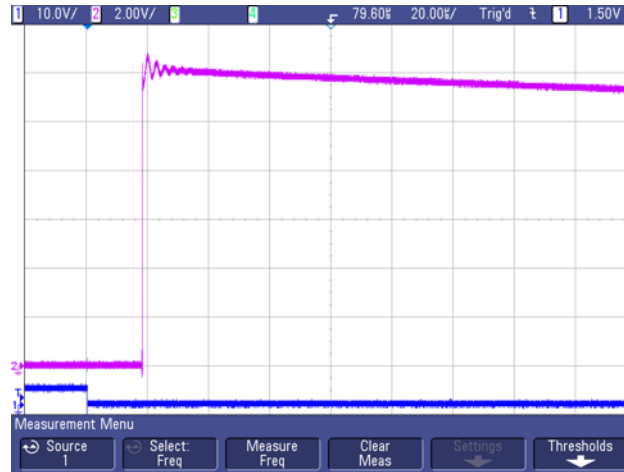
图 14. Input Current vs. Positive Applied VBATT



### 3.2.2.2 Motor Drive A Testing

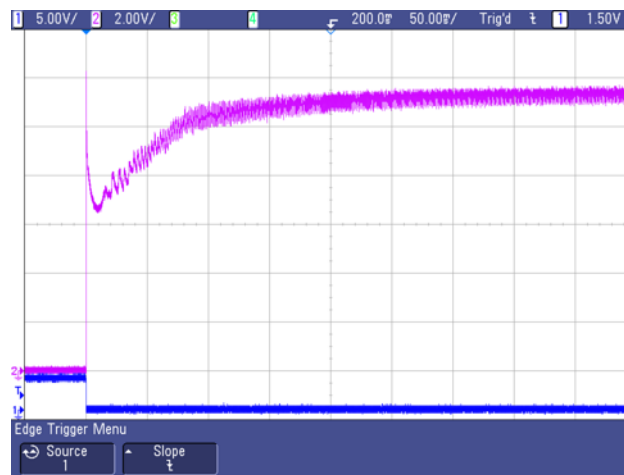
The Drive A circuit uses the DRV8703-Q1 to implement a relatively high-current motor drive. This circuit was tested with the windshield wiper motor described in 表 3. Further functional testing was performed using the power seat tilt motor.

图 15. DRV8703-Q1 Motor Start Delay



Channel 1 is the pushbutton signal, channel 2 is the voltage applied to the motor. The delay between button push and application of motor voltage is about 20 ms. The motor voltage increases rapidly to about 12 V, with a small ringing on the rising edge. The motor voltage of approximately 12 V indicates there is not a significant voltage drop across the active full-bridge MOSFETs, due to the low  $R_{DS(ON)}$  of the MOSFETs selected.

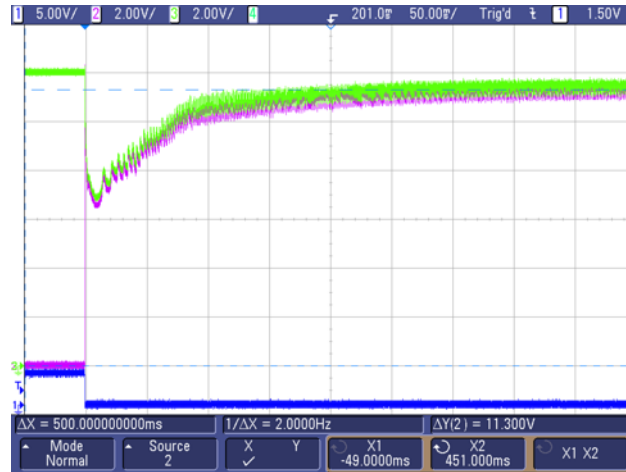
图 16. DRV8703-Q1 Motor Start Detail



The bench supply is limited to 10 A, so that when the motor voltage is first applied, the current exceeds the supply. The motor in this case has a DC resistance of  $0.68 \Omega$ , so the motor voltage drops to about 6.8 V before the motor begins to turn. As the motor begins to turn, the back EMF increases, and the motor voltage increases to a steady level at about 11.3 V with some observable ripple. The motor used for this test has a steady-state current of about 5 A. Losses in the test cables between the supply and the TIDA-020008 board account for most of the difference between the nominal 12-V supply level and the observed steady-state motor voltage.

This power supply droop is illustrated in 图 17, where the supply to the TIDA-020008 board has been added on Channel 3. The voltage losses on the board (between the supply VBATT and the motor voltage) are due to the reverse-battery protection FET and the high-side driver FET.

图 17. DRV8703-Q1 Motor Start Showing Supply Droop



The current feedback accuracy of the DRV8703-Q1 is especially important if this signal is used to determine when the motor has encountered a high-current state, for example a stall condition. The combination of scale factor accuracy and offset determine the overall accuracy of the motor current sense signal. 图 18 shows the linearity of the Isense signal. This plot shows the Isense signal for two different boards. In both cases the slope of the line is about 0.434 V per amp. The offset value varies between the two boards. In normal operation, designer may choose to sample the Isense signal during the system initialization, to determine the zero-current offset of the Isense signal. During normal operation, this offset value can be subtracted from all subsequent Isense measurements to determine the motor current with high accuracy.

图 18. Drive A Isense Signal Voltage vs. Current

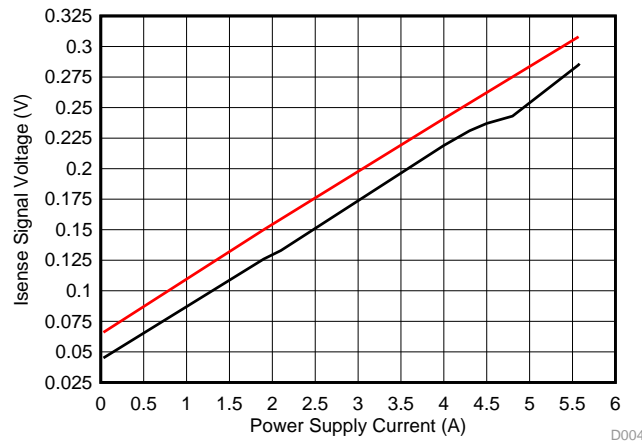


图 19 shows the motor current when Drive A is activated. Channel 1 is the switch input signal which transitions when the button is pressed. Channel 2 is the voltage across the current sense resistor. Channel 3 is the voltage on I\_SENSE reported back to the microcontroller. After accounting for offset, the amplified (gain = 10) I\_SENSE signal has the same amplitude and shape as the voltage on the resistor. The initial high current is when the voltage is first applied to the stationary motor, and thus no back EMF is available to reduce the current.

图 19. DRV8703-Q1 Motor Start Current Signals

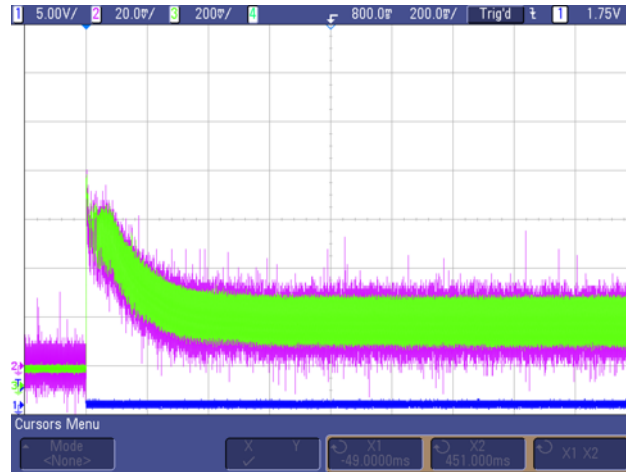
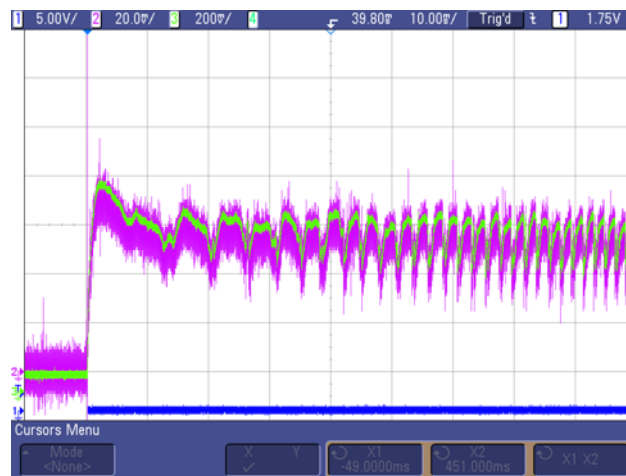


图 20 显示的是电机启动期间的电流信号放大视图。电流纹波在通道 3 的 I\_Sense 信号上更容易看到，它是通道 2 的信号（跨电流检测电阻的电压）的放大版本。

图 20. DRV8703-Q1 电流检测保真度



将电流检测信号直接在检测电阻上，与经过 DRV8703-Q1 电流检测放大器后的信号进行比较，显示放大后的 I\_SENSE 信号（通道 3）与电机检测电阻上的电压（通道 2）相比，没有表现出任何显著的时间延迟。检测电阻上的信号表现出高度的噪声，因为示波器设置处于最低可用范围，为 20 mV 每格。

### 3.2.2.3 Motor Drive B Testing

One application for the Drive B design, based on the DRV8873-Q1, is to control the height of a motorized headrest. 图 21 shows an example of a power headrest assembly. In this assembly, a 12-V brushed DC motor is connected through a gear system which drives a slider rack up and down. The gear system changes the axis of rotation by 90 degrees, allowing the motor to be mounted horizontally. The gears also reduce the speed of rotation by a factor of about 20, with a corresponding increase in applied torque of about 20. A small circuit board in the power headrest assembly includes a Hall effect sensor which senses the magnetic field produced by a rotating permanent magnet. This provides a feedback signal related to the rotational position of the motor shaft.

图 21. Headrest Mechanism

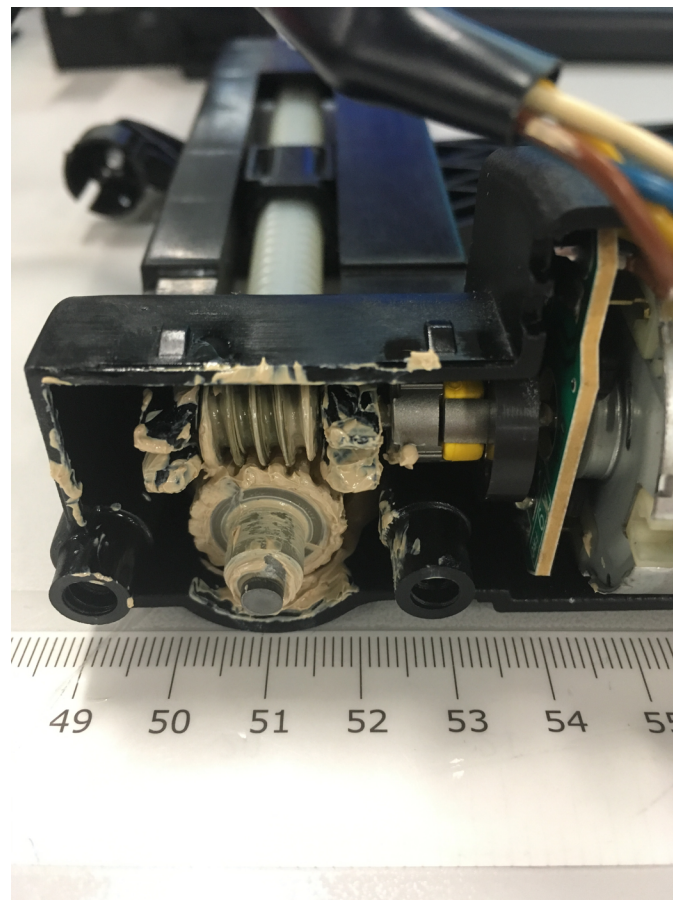
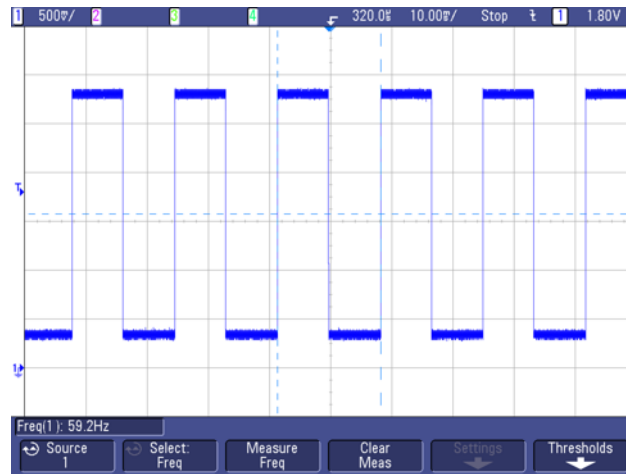


图 22 shows the output from the Hall effect sensor mounted in the power headrest assembly. Each transition indicates the motor shaft has rotated to a bring the magnet to a position such that the magnetic field has changed polarity. So the frequency of the Hall effect sensor signal is directly related to the motor speed.

图 22. Headrest Hall Effect Signal



The frequency of the Hall effect sensor signal is used to measure the motor speed for various levels of applied supply voltage VBATT. 图 23 shows the results of this testing. As expected, the speed increases as the applied VBATT voltage level increases. The relationship is relatively linear across the expected range of operation, with some variation due to mechanical factors such as the friction of the gears.

图 23. Headrest Hall Effect Signal Frequency vs. Applied VBATT Voltage

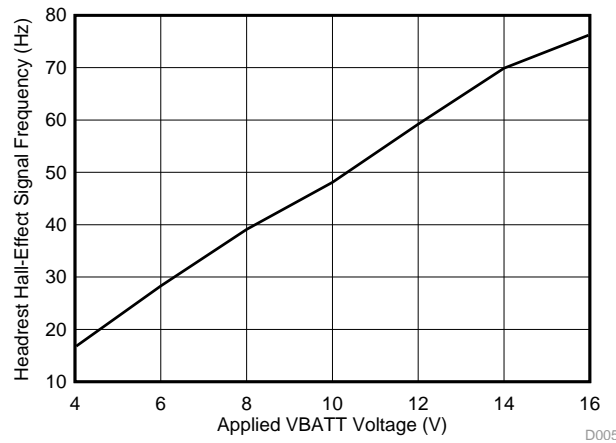
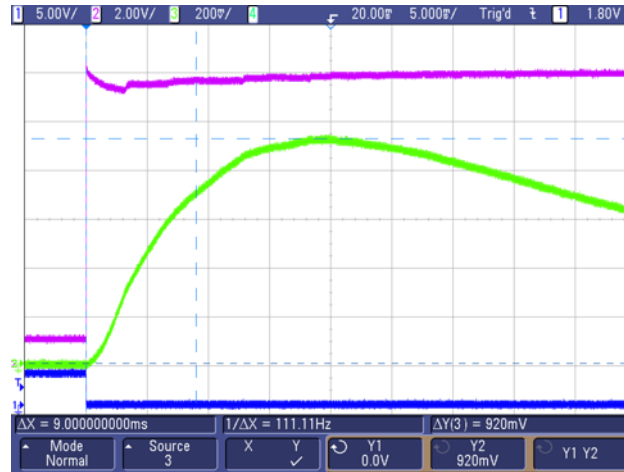


图 24 shows oscilloscope traces of the Drive B circuit when the headrest motor begins motion as commanded by the microcontroller in response to a user button push. Channel 1 is the signal from Switch 5, Channel 2 is the high-side of the motor voltage, and Channel 3 is the current sense signal to the MCU on connector pin J4-16.

The value of 1 kΩ for R14 (in this case) and scale factor of 1125 A/A on the IPROP signal gives a scale factor of 1.125 A of motor current per Volt of signal on ISense8873. The measured maximum value of 920 mV of ISENSE (after the MUX) indicates the maximum motor current is:

$$0.920 \text{ V} \times 1.125 \text{ A} / \text{V} = 1.04 \text{ A of motor current}$$

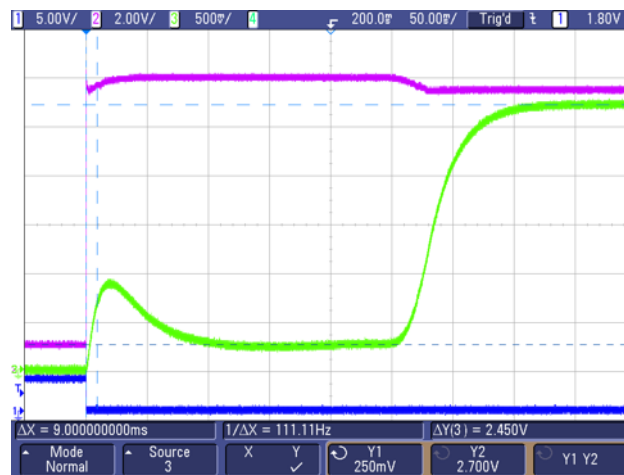
图 24. Headrest Motion Start Using DRV8873-Q1



As the motor accelerates, the back EMF produced by the motor increases, reducing the current through the motor. This is seen in the current trace (Channel 3) when the ISENSE signal amplitude reduces below the maximum value.

Another case of interest is to observe these signals when the headrest mechanism reaches a mechanical stop at the end of its travel, causing the headrest motor to stall. 图 25 illustrates this. Channel 1 is the signal from Switch 5, Channel 2 is the high-side of the motor voltage, and Channel 3 is the current sense signal to the MCU on connector pin J4-16.

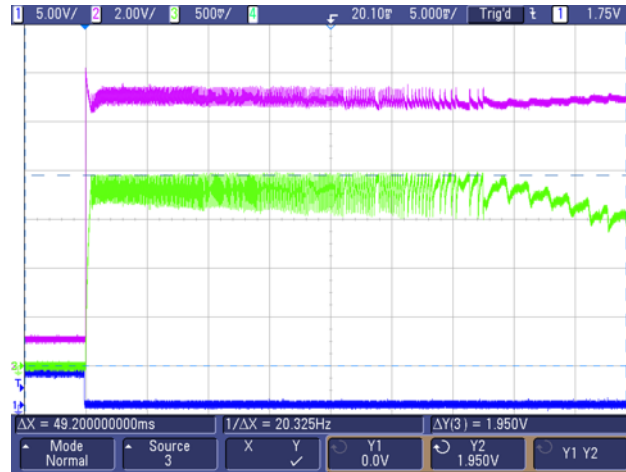
图 25. DRV8873-Q1 Motor Driving Headrest Lift Showing Motor Stall



After the initial motor acceleration, the motor current signal drops to about 250 mV, indicating the typical running current of about 280 mA. When the end of travel is reached, the motor stalls, and the current signal increases to about 2.7 V, corresponding to a stall current of 3.04 A. Since this stall current is less than the default current limit of 6.5 A, the DRV8873-Q1 does not limit the current. If designers want to set a lower current limit for this drive, it is adjustable as a DRV8873-Q1 register setting.

To see how the DRV8873-Q1 design performs with a higher-current motor, a window lifter motor is connected to the Drive B circuit. This motor has a winding resistance of 1.2 Ω, so that the stall current is about 10 A with a 12-V supply. The operation of the DRV8873-Q1 current limit can be observed at a default setting of 6.5 A.

图 26. DRV8873-Q1 Motor Start Current Limiting



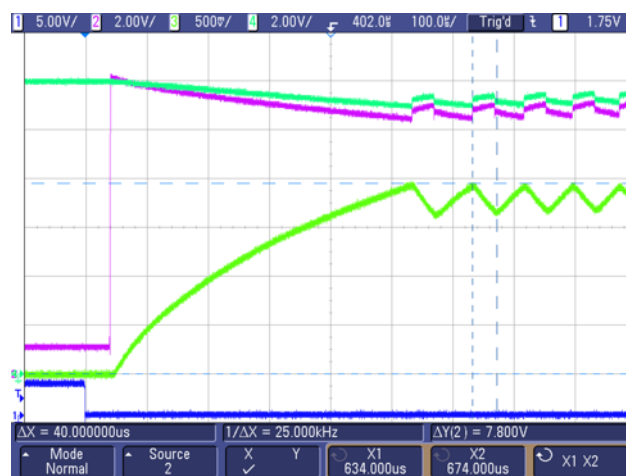
The DRV8873-Q1 current limit threshold is set to 6.5 A  $\pm$ 1 A when ITRIP\_LVL is set to 10b. The value of 330  $\Omega$  for R14 (in this case) and scale factor of 1125 A/A on the IPROP signal gives a scale factor of 3.4 A of motor current per volt of signal on ISense8873. The measured maximum value of 1.95 V of ISENSE (after the MUX) indicates the current is limiting at a value of:

$$1.95 \text{ V} \times 3.4 \text{ A/V} = 6.63 \text{ A of motor current}$$

As the motor accelerates, the back EMF produced by the motor increases, reducing the current through the motor. This is seen in the current trace (Channel 3) when the ISENSE signal amplitude reduces below the limiting value.

图 27 shows a detail of the window lifter motor start-up using the DRV8873-Q1 design. The switch input is on Channel 1. The motor voltage on Channel 2 responds after about 50 microseconds, increasing to about 12 V. The motor current signal on channel 3 (ISense8873) begins to increase when the motor voltage is applied, increasing according to the motor electrical time constant  $L_m/R_m$ . When the current limit value is reached, the full-bridge drive is put into slow-decay by enabling both high-side drivers. The motor current reduces during this period, the duration of which is set by the TOFF bits. In this example, the TOFF bits are set to the default value of 01b, giving an off time of 40 microseconds, as indicated by the cursors.

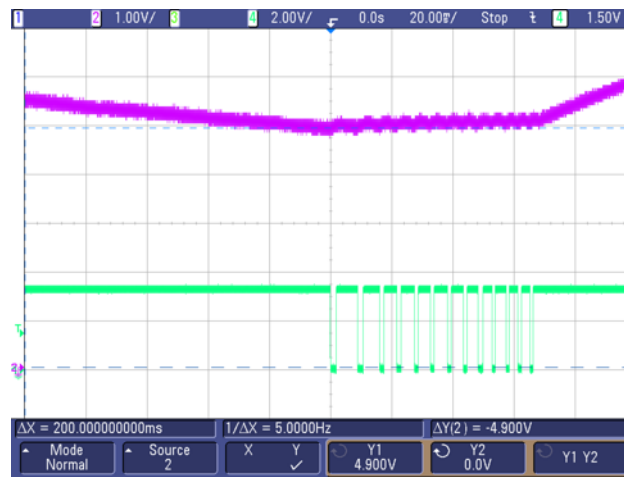
图 27. DRV8873-Q1 Motor Start Current Limiting Detail



The motor voltage reduces as the current increases, so that when the current limit of 6.63 A is reached, the motor voltage has dropped to about 10.5 V. The drop of 1.5 V indicates a resistance of about 225 mΩ. The DRV8873-Q1 specifies a typical on-resistance of 75 mΩ for the high-side FET and the low-side FET. This resistance accounts for the drop between the supply voltage VBATT shown on Channel 4 and the voltage on the high-side of the motor on Channel 2. The drop in VBATT is due to the test bench cable resistance between the bench power supply and the TIDA-020008 board TB1-2 VBATT input.

In the test in 图 28, the current limit for the bench power supply was set to slightly less than the average running current for the motor, thus causing the voltage at VBATT to droop when the motor current exceeds the current limit. Channel 2 shows the VBATT signal drooping to about 4.9 V and then increasing, as the headrest adjustment travels through a range of higher-than-average friction.

图 28. Drooping VBATT Causes OK\_8873 Signal to Go Low

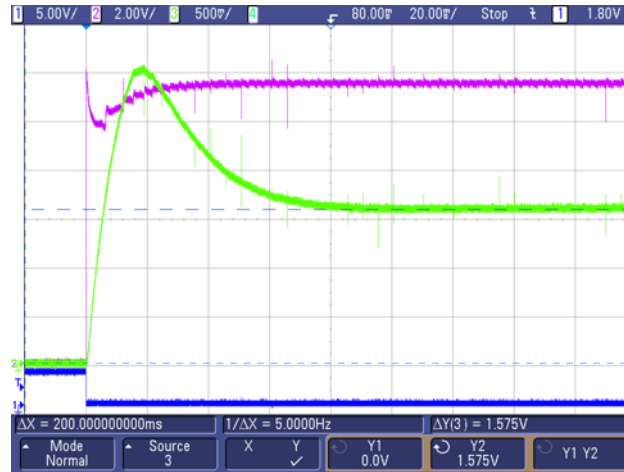


Channel 4 shows the reaction of the OK\_8873 signal to the drooping VBATT. When the motor current first droops to about 4.9 V, the DRV8873-Q1 FAULT open-drain output signal activates, pulling the OK\_8873 signal to a logic low level.

### 3.2.2.4 Drive C Testing

The Drive C circuit uses one channel of the U8 smart high-side switch TPS2H160-Q1 to implement a unidirectional motor drive, as 图 4 shows. For testing this circuit, a lumbar support pump is used as the load; this pump motor is described in 表 3. 图 29 shows an oscilloscope plot of the signals during start up of the lumbar pump motor.

图 29. Lumbar Pump Start Up



Channel 1 shows the signal on SWITCH1 going low when the button is pushed. Channel 2 shows the motor voltage; Channel 3 shows the ISense\_HSS signal which corresponds to the current through the high-side switch to the pump motor.

Initially the motor current reaches a peak when the motor is turning slowly, and thus has only a small back EMF. After the motor accelerates to a constant speed, the motor current signal is steady at a level of about 1.6 V.

The scale factor for the ISense\_HSS signal is about 1 V/A of output current, so this signal indicates the steady-state pump current is about 1.6 A.

图 30 shows an oscilloscope plot of the signals when the lumbar pump motor is turned off.

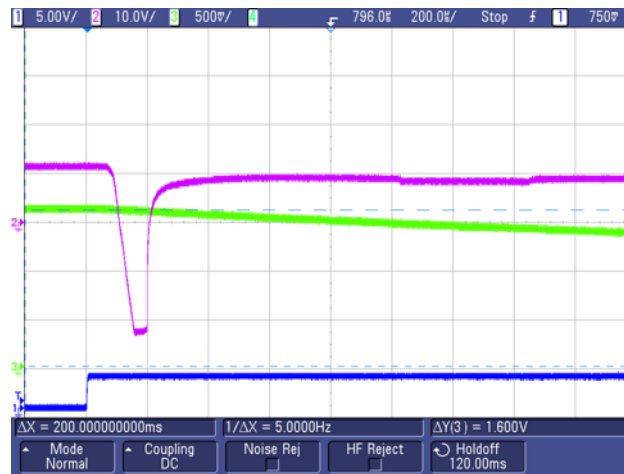
图 30. Lumbar Pump Turn Off



When the signal on Channel 1 indicates the *Lumbar Inflate* function has turned off, the TPS2H160A-Q1 OUT2 channel turns off, disconnecting the lumbar pump motor from the 12-V supply. The motor voltage on Channel 2 reduces and the motor current begins to reduce. Due to the inductance of the pump motor winding, the motor current does not immediately drop to zero, but decays as the energy stored in the windings dissipates. The motor voltage exhibits a sharp negative transition, and then shows the effects of the motor generating voltage as it continues to turn. The ripples in the motor voltage indicate the motor turning, obviously slowing until coming to a halt at the end of this plot.

图 31 shows an expanded view of the pump motor turn off signals.

图 31. Detail of Lumbar Pump Turn Off

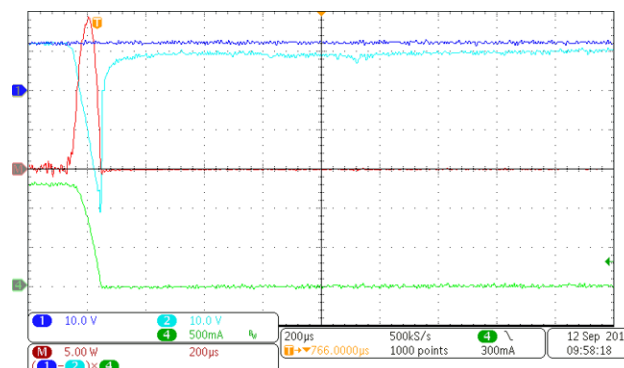


A detail of the motor voltage transition on lumbar pump turn off shows the amplitude and duration of the inductive *kick* caused by turning off the motor. The duration of the negative pulse is about 100 microseconds. The negative pulse is clamped at about 23 V. Zener diode D5 has a nominal breakdown point of 21 V; the remainder of the voltage drop is due to the blocking diode D6.

To determine if the clamping circuit formed by D5 and D6 is necessary, the diodes were removed, and 图 32 shows the signals during solenoid turn-off. In this oscilloscope plot, Channel 1 is the VBATT supply voltage at a nominal 12-V level. Channel 2 is the voltage across the solenoid windings. Channel 4 is the current through the solenoid windings, measured using a current probe. The fourth channel (M) is a calculated power on the TPS2H160-Q1 circuit, found by taking the voltage difference between the supply and the winding, multiplied by the current.

As expected, with no external clamping diode, the voltage across the motor winding transitions to a negative voltage, reaching about -32 V. During this time, the current through the motor coil is decaying towards zero. The power which must be dissipated by the TPS2H160-Q1 internal circuits peaks at about 19 W, with a duration of about 1 ms. Approximating the power signal as a triangle with height 19 W and base 1 ms, the integration of the power signal gives an energy of 9.5 mJ.

图 32. Motor Demagnetization for the Lumbar Pump

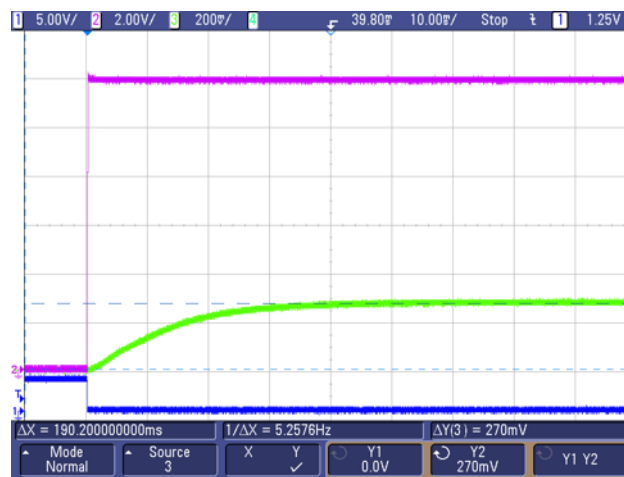


The TPS2H160-Q1 specifies an absolute maximum of 40 mJ for "Inductive load switch-off energy dissipation, single pulse, single channel", so this energy that must be dissipated each time the lumbar pump motor is turned off is significantly less than the specified value. Designers can use the TPS2H160-Q1 for this application without the need for protection diodes D5 and D6, unless the motor is significantly larger than the model used for testing.

### 3.2.2.5 Drive D Testing

The Drive D circuit is based on a unidirectional high-side switch as 图 4 shows. This circuit was tested using the lumbar valve as a load. This valve includes a solenoid with spring return, and a diode to clamp the inductive spike caused by turning off the current to the solenoid coil.

图 33. Lumbar Valve Turn On



Channel 1 is the button which switches to a low state when depressed. Channel 2 is the voltage to the solenoid windings, quickly reaching a value of 12 V after the button is depressed. Channel 3 is the current sense signal which originates in the TPS2H160-Q1 current mirror, is selected through the SN74LV4051A-Q1 analog MUX, and is filtered by the RC low-pass formed by R24 and C27. With an R24 value of 10 k $\Omega$  and a C27 value of 1  $\mu$ F, the RC time constant is 10 ms, which is reflected in the response of the current signal. The amplitude of the steady-state current signal is about 270 mV. As discussed in 节 2.4.3, the scale factor is about 1 V/A, so this represents a steady-state current of 270 mA to activate the lumbar valve solenoid.

图 34 shows the waveforms as the lumbar valve is turned off.

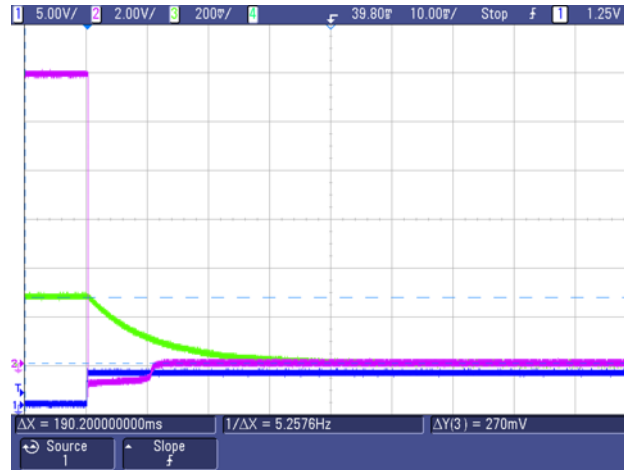
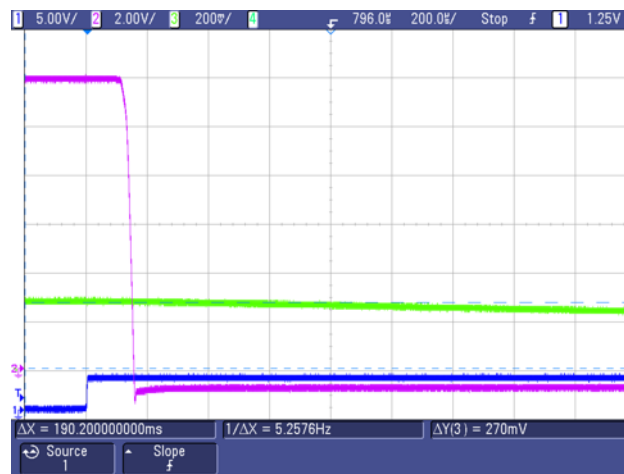
**图 34. Lumbar Valve Turn Off**


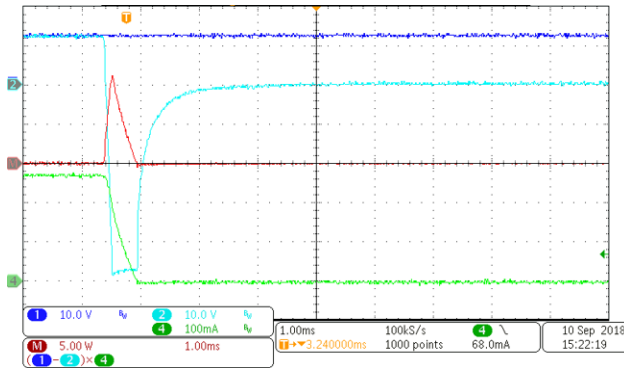
图 35 shows an expanded view of the signal waveforms during lumbar valve solenoid turn off. The solenoid voltage on Channel 2 transitions to a negative value due to the inductive energy stored in the solenoid windings. The negative voltage level is clamped to about  $-0.7\text{ V}$  by the external diode supplied with the lumbar valve.

**图 35. Detail of Lumbar Valve Turn Off**


To determine if the external diode supplied with the solenoid valve is necessary, the external diode was removed, and 图 36 shows the signals during solenoid turn-off. In this oscilloscope plot, Channel 1 is the VBATT supply voltage at a nominal 12-V level. Channel 2 is the voltage across the solenoid windings. Channel 4 is the current through the solenoid windings, measured using a current probe. The fourth channel (M) is a calculated power on the TPS2H160-Q1 circuit, found by taking the voltage difference between the supply and the winding, multiplied by the current.

As expected, with no external clamping diode, the voltage across the solenoid winding transitions to a negative voltage, reaching about  $-48\text{ V}$  where it is clamped by the internal protection circuits of the TPS2H160-Q1. During this time, the current through the solenoid coil is decaying towards zero. The power which must be dissipated by the internal protection circuits peaks at about  $12\text{ W}$ , with a duration of about  $1\text{ ms}$ . Approximating the power signal as a right triangle with height  $12\text{ W}$  and base  $1\text{ ms}$ , the integration of the power signal gives an energy of  $6\text{ mJ}$ .

图 36. Solenoid Demagnetization During Lumbar Valve Turn Off

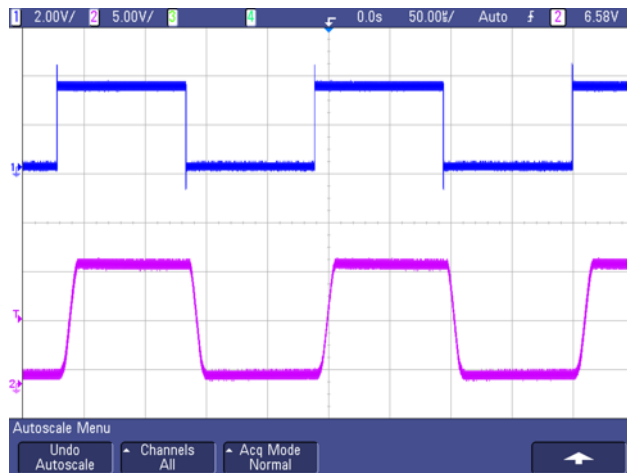


The TPS2H160-Q1 specifies an absolute maximum of 40 mJ for "Inductive load switch-off energy dissipation, single pulse, single channel", so this energy that must be dissipated each time the solenoid valve is turned off is significantly less than the specified value. Designers can therefore use the TPS2H160-Q1 for this application without the need for external protection diodes.

### 3.2.2.6 LIN Transceiver Operation

图 37 shows the signals during LIN transmitter operation. Channel 1 is the input to the transceiver on the TXD signal, changing state with a bit width of about 100 microseconds. Channel 2 is the LIN bus signal which responds to the TXD signal.

图 37. LIN Transceiver Operation Signals



At this scale, there is no observable time delay between transitions on the TXD pin and transitions on the LIN pin. The controlled slope of the LIN bus signals is also apparent. For this measurement, a 1-kΩ resistor to VBATT was applied to the LIN bus line, as would normally occur when connected to a master node. See also

## 4 Design Files

### 4.1 Schematics

To download the schematics, see the design files at [TIDA-020008](#).

### 4.2 Bill of Materials

To download the bill of materials (BOM), see the design files at [TIDA-020008](#).

### 4.3 PCB Layout Recommendations

#### 4.3.1 Layout Prints

To download the layer plots, see the design files at [TIDA-020008](#).

### 4.4 Altium Project

To download the Altium Designer® project files, see the design files at [TIDA-020008](#).

### 4.5 Gerber Files

To download the Gerber files, see the design files at [TIDA-020008](#).

### 4.6 Assembly Drawings

To download the assembly drawings, see the design files at [TIDA-020008](#).

## 5 Software Files

To download the software files, see the design files at [TIDA-020008](#).

## 6 Related Documentation

1. Texas Instruments, [DRV870x-Q1 Automotive H-Bridge Gate Driver Data Sheet](#)
2. Texas Instruments, [DRV8873-Q1 Automotive H-Bridge Motor Driver Data Sheet](#)
3. Texas Instruments, [TPS2H160-Q1 Dual-Channel Smart High-Side Switch Data Sheet](#)
4. Texas Instruments, [TPS7B82-Q1 High-Voltage Ultralow- \$I\_q\$  Low-Dropout Regulator Data Sheet](#)
5. Texas Instruments, [TPS22810-Q1 Load Switch with Thermal Protection Data Sheet](#)
6. Texas Instruments, [SN74LV4051A-Q1 8-Channel Analog Multiplexer/Demultiplexer Data Sheet](#)
7. Texas Instruments, [TLIN1029-Q1 LIN Transceiver with Dominant State Timeout Data Sheet](#)
8. Texas Instruments, [Understanding IDRIVE and TDRIVE in TI Smart Gate Drivers Application Report](#)
9. Texas Instruments, [LIN Protocol and Physical Layer Requirements Application Report](#)

## 6.1 商标

E2E, LaunchPad, BoosterPack, Code Composer Studio are trademarks of Texas Instruments. Altium Designer is a registered trademark of Altium LLC or its affiliated companies. All other trademarks are the property of their respective owners.

## 7 About the Author

**CLARK KINNAIRD** is a systems applications engineer at Texas Instruments. As a member of the Automotive Systems Engineering team, Clark works on various types of end-equipment, especially in the field of body electronics, creating reference designs for automotive manufacturers. Clark earned his bachelor of science and master of science in engineering from the University of Florida, and his Ph.D. in electrical engineering from Southern Methodist University.

## 重要声明和免责声明

TI 均以“原样”提供技术性 & 可靠性数据（包括数据表）、设计资源（包括参考设计）、应用或其他设计建议、网络工具、安全信息和其他资源，不保证其中不含任何瑕疵，且不做任何明示或暗示的担保，包括但不限于对适销性、适合某特定用途或不侵犯任何第三方知识产权的暗示担保。

所述资源可供专业开发人员应用 TI 产品进行设计使用。您将对以下行为独自承担全部责任：(1) 针对您的应用选择合适的 TI 产品；(2) 设计、验证并测试您的应用；(3) 确保您的应用满足相应标准以及任何其他安全、安保或其他要求。所述资源如有变更，恕不另行通知。TI 对您使用所述资源的授权仅限于开发资源所涉及 TI 产品的相关应用。除此之外不得复制或展示所述资源，也不提供其它 TI 或任何第三方的知识产权授权许可。如因使用所述资源而产生任何索赔、赔偿、成本、损失及债务等，TI 对此概不负责，并且您须赔偿由此对 TI 及其代表造成的损害。

TI 所提供产品均受 TI 的销售条款 (<http://www.ti.com.cn/zh-cn/legal/termsofsale.html>) 以及 [ti.com.cn](http://www.ti.com.cn) 上或随附 TI 产品提供的其他可适用条款的约束。TI 提供所述资源并不扩展或以其他方式更改 TI 针对 TI 产品所发布的可适用的担保范围或担保免责声明。

邮寄地址：上海市浦东新区世纪大道 1568 号中建大厦 32 楼，邮政编码：200122  
Copyright © 2018 德州仪器半导体技术（上海）有限公司

## 重要声明和免责声明

TI 均以“原样”提供技术性 & 可靠性数据（包括数据表）、设计资源（包括参考设计）、应用或其他设计建议、网络工具、安全信息和其他资源，不保证其中不含任何瑕疵，且不做任何明示或暗示的担保，包括但不限于对适销性、适合某特定用途或不侵犯任何第三方知识产权的暗示担保。

所述资源可供专业开发人员应用 TI 产品进行设计使用。您将对以下行为独自承担全部责任：(1) 针对您的应用选择合适的 TI 产品；(2) 设计、验证并测试您的应用；(3) 确保您的应用满足相应标准以及任何其他安全、安保或其他要求。所述资源如有变更，恕不另行通知。TI 对您使用所述资源的授权仅限于开发资源所涉及 TI 产品的相关应用。除此之外不得复制或展示所述资源，也不提供其它 TI 或任何第三方的知识产权授权许可。如因使用所述资源而产生任何索赔、赔偿、成本、损失及债务等，TI 对此概不负责，并且您须赔偿由此对 TI 及其代表造成的损害。

TI 所提供产品均受 TI 的销售条款 (<http://www.ti.com.cn/zh-cn/legal/termsofsale.html>) 以及 [ti.com.cn](http://www.ti.com.cn) 上或随附 TI 产品提供的其他可适用条款的约束。TI 提供所述资源并不扩展或以其他方式更改 TI 针对 TI 产品所发布的可适用的担保范围或担保免责声明。

邮寄地址：上海市浦东新区世纪大道 1568 号中建大厦 32 楼，邮政编码：200122  
Copyright © 2018 德州仪器半导体技术（上海）有限公司